Research Article | Vol. 28, No. 20 / 28 September 2020 / Optics Express 29469
Optics EXPRESS

Sequential high power laser amplifiers for gravitational wave detection

NINA BODE,* FABIAN MEYLAHN, AND BENNO WILLKE

Max-Planck-Institut für Gravitationsphysik (Albert-Einstein-Institut) and Leibniz Universität Hannover, Callinstr. 38, 30167 Hannover, Germany
*nina.bode@aei.mpg.de

Abstract: Advanced gravitational wave detectors require highly stable, single mode, single frequency and linear polarized laser systems. They have to deliver an output power of ~200 W and need to provide suitable actuators for further stabilization via fast, low noise feedback control systems. We present such a laser system based on sequential Nd:YVO_4 amplifiers and its integration into a typical laser stabilization environment. We demonstrate robust low noise operation of the stabilized amplifier system at 195 W, which makes it a viable candidate for use in gravitational wave detectors.

1. Introduction

With the first detection of gravitational waves in September 2015 [1] a new field of astronomy opened up in which several additional detections have been made since then.

After the second observing run the gravitational wave detector network, consisting of two advanced LIGO (aLIGO) detectors in the United States [2], the advanced Virgo detector in Italy [3] and the GEO600 detector in Germany [4], published the first catalogue of gravitational waves [5]. All gravitational wave detectors in this network are complex Michelson interferometers with arm lengths of 600 m for GEO600 and several kilometers for the other detectors. Most of the measured gravitational waves were generated by merging black holes and one was produced by a binary neutron star system. The good sky localization of the neutron star merger by the gravitational wave detectors allowed telescopes to identify the host galaxy of the event by measuring the electromagnetic counterparts of the gravitational wave signal. That triggered an observation campaign with more than 70 telescopes on ground and in space [6].

The sensitivity of gravitational wave detectors is limited by various noise sources that need to be suppressed as much as possible. At frequencies above ~200 Hz quantum noise, to be more precise photon shot noise, is the limiting noise source for these detectors. This noise is a result of the Poisson distribution of the photons in a laser beam and can mask gravitational wave signals on the interferometer output. The relative shot noise scales anti-proportional to the square root of the laser power and thus high power laser sources are required. In this paper we present such a laser source adequate for future gravitational wave detector upgrades.

In the first section we show the functionality and characteristics of a laser amplifier system based on the neoVAN-4S-HP, a solid state laser amplifier manufactured by the company neoLASE.

In the second section the integration of two of those amplifiers in an existing pre-stabilization environment is demonstrated. We achieved an output power level of 114 W for one neoVAN-4S-HP [7] and 195 W for two neoVAN-4S-HP amplifiers in series. The system was fully characterized with two diagnostic breadboards [8,9] and long term measurements were performed.

In the third section we show how the neoVAN-4S-HP amplifiers perform with frequency and power stabilized seed beam, respectively.

At the end of this paper we summarize our results briefly and discuss if the amplifiers can be implemented behind the stabilization loops, or must be part of them.

#401826
Journal © 2020

Optics EXPRESS

2. Laser system

The different laser components and stabilization elements used in our experiment are arranged according to the simplified experimental setup shown in Fig. 1.

The low noise, single mode and single frequency seed laser is a copy of the original enhanced LIGO (eLIGO [10]) laser [11]. It consists of a non-planar ring oscillator laser (NPRO) [12] operating at a wavelength of 1064 nm and an output power of 2 W followed by a Nd:YVO_4 amplifier (amp 1) with a maximal output power of 35 W. This kind of laser system has proven its reliability over years in the GEO600 gravitational wave detector, in the eLIGO detectors and as a seed laser for the aLIGO pre-stabilized laser system [13]. In our experiment the output power of this seed laser was reduced to 27 W to optimize the higher order mode content (HOM) to 2.7%. The seed beam gets amplified in two sequential neoVAN-4S-HP amplifiers at different positions in the setup. Each of these amplifiers consist of four Nd:YVO_4 crystals in series as shown in Fig. 2. Each crystal is pumped by a laser diode operating at a wavelength of 878 nm with a maximum power of 65 W. The diodes are wavelength stabilized via volumetric Bragg gratings. The light of the pump diodes is send via fibers to the amplifier module, where lenses focus the pump light, through dicroic mirrors, into the amplifier crystals. The pump diodes and their electronics, as well as the Nd:YVO_4 crystals are water cooled. When the seed laser passes the pumped crystal it gets amplified by stimulated emission at the seed laser wavelength. For sufficiently high seed power levels the amplifier is saturated and up to 95 W of power at a wavelength of 1064 nm could be extracted from a single neoVAN-4S-HP amplifier.

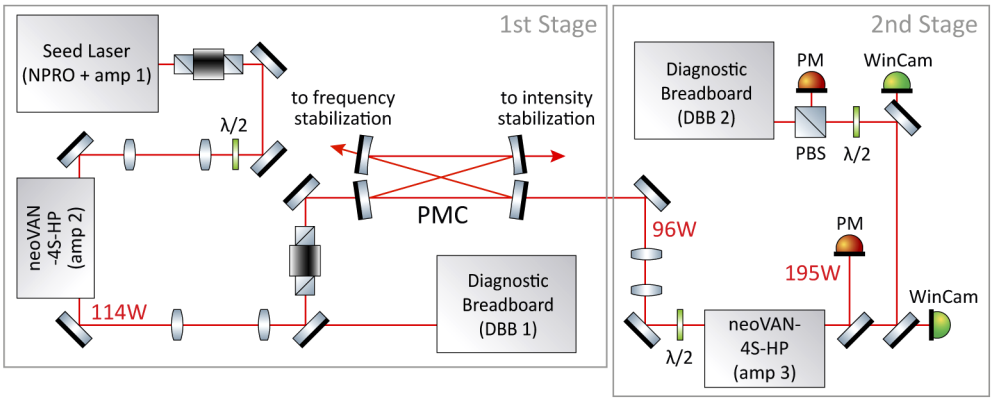

Fig. 1. The laser system consists of a first and a second stage. The first stage contains a diagnostic breadboard (DBB 1) to characterize the beam coming from the first neoVAN-4S-HP amplifier. The pre-mode cleaner (PMC) performs spatial filtering to the laser beam. One of its low power outputs is guided to an ultra-stable in-vacuum cavity (omitted in the diagram for clarity) that serves as a reference for the frequency stabilization. The second low power output is send to several sensing photo diodes (omitted for clarity as well) for the intensity stabilization. The output beam of the second neoVAN-4S-HP in the second stage is characterized with a second diagnostic breadboard (DBB 2) and several cameras (WinCam) and power detectors (PM).

The first neoVAN-4S-HP, labeled amp 2 in Fig. 1, was located behind the seed laser. A small fraction of the amplified beam was send to a diagnostic bread board (DBB 1). The diagnostic breadboard is a device that combines several photo detectors, automatically steerable mirrors and a triangular optical cavity to, fully automatically, measure the relative power noise, frequency noise, relative beam pointing noise and the HOM of the inserted laser beam [8].

The main fraction of the beam coming from amp 2 passed a pre-mode cleaner (PMC) [14] that performs some spatial filtering of the laser beam and provides two low power beam samples

Optics EXPRESS

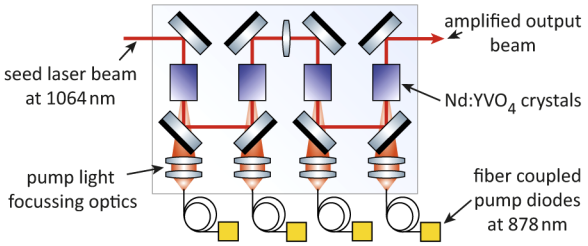

Fig. 2. Setup of the neoVAN-4S-HP amplifiers. The seed laser beam passes four Nd:YVO_4 crystals in series. Fiber coupled diodes, at a wavelength of 878 nm with a maximal power of 65 W, are used to pump the crystals such that a power extraction of up to 95 W is achievable.

that can be used for frequency- and power stabilization. The diagnostic breadboards as well as the pre-mode cleaners and the stabilization loops are identical to the ones used in the aLIGO pre-stabilized laser systems [13].

This first stage of the laser system was characterized in [7]. It delivered a laser power of 114 W in front and more than 100 W in transmission of the PMC.

Up to 96 W from the beam spatially filtered by the PMC served as seed for the second neoVAN-4S-HP (amp 3) in the second stage of our setup. This high power seed laser beam with an almost perfect TEM_{00} spatial mode is an optimal source to characterize the third amplifier. In addition to the high spatial purity we can stabilize the power and frequency of this seed beam to analyze the noise added by a neoVAN-4S-HP to a low noise seed beam. The second diagnostic bread board (DBB 2) was used to characterize the output beam of the third amplifier. To avoid light from amp 3 travelling backwards into amp 2 we installed an additional Faraday isolator in front of the PMC. The maximal output power that we measured behind the third amplifier was 195 W with a higher order mode content <14% and a polarization extinction ratio >18 dB. This exceeds the laser power that was available in the last LIGO/Virgo observation run of 70 W (LIGO) and 100 W (Virgo, [15]) and could provide the originally anticipated 165 W in transmission of the PMC to reach the advanced LIGO design sensitivity [16].

3. Free running characterization

In this section we present the characterization of the laser system with the power and frequency stabilization system not engaged.

Gain measurements of both neoVAN-4S-HP amplifiers were taken, by varying their seed power at a constant pump power level (see Fig. 3). Half wave plates together with a polarizing beam splitter and a thin film polarizer were used to adjust the seed power for amp 2 and amp 3, respectively. By subtracting the seed power from the output power we calculated the extracted power. For both amplifiers, the extracted power, plotted in red, first increases with the seed power and then saturates to a nearly fixed value. For the first neoVAN-4S-HP (amp 2) the extracted power is $\sim$ 80 W for seed powers $\geq$ 5 W (see Fig. 3(a)). The almost constant difference of output power, plotted in blue, and PMC transmission, plotted in green, shows that the mode shape doesn't change significantly. The mode matching and alignment to amp 2 was initially optimized for a seed power of 27 W and not changed afterwards.

The measurements of the second neoVAN-4S-HP (amp 3) are shown in Fig. 3(b). It was performed after the long term measurement shown in Fig. 4, hence a maximal output power of about 186 W was reached in this plot. The output power is shown in blue and the extracted power is shown in red. For seed powers $\geq$ 20 W the extracted power is $\sim$ 95 W. DBB 2 measurements of the higher order mode content (plotted in pink) for increasing seed power show an increase of the HOM content from about 6% to 11%. Here the mode matching and alignment to amp 3

Optics EXPRESS

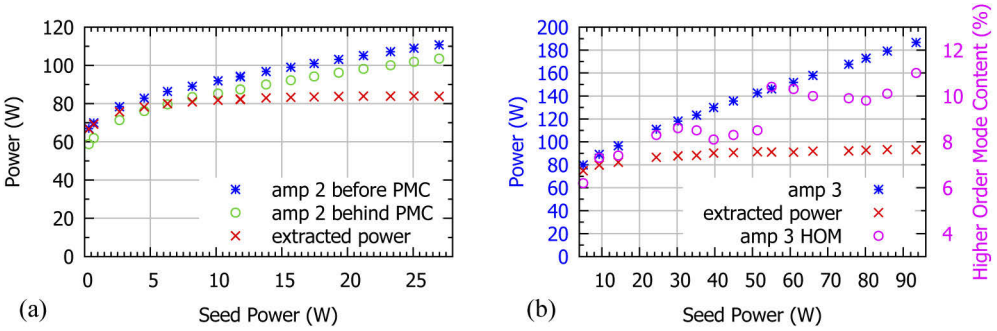

Fig. 3. (a) Amplified power, PMC transmission and extracted power as a function of the seed power of the first neoVAN-4S-HP. The extracted power settles to about 80 W. (b) Amplified power, extracted power and higher order mode content as a function of the seed power of the second neoVAN-4S-HP. The extracted power settles to about 95 W.

was optimized for the maximal measured seed power and not changed during the seed power variations. The orientation of the half wave plate in front of the amplifier, however, had to be optimized during the measurement sequence as the amplifier crystals are birefringent and thus the cross section for stimulated emission is strongly dependent on changes in the input polarization. Such changes were caused by absorption in the half wave plate leading to a power dependent temperature and hence, a power dependent retardation.

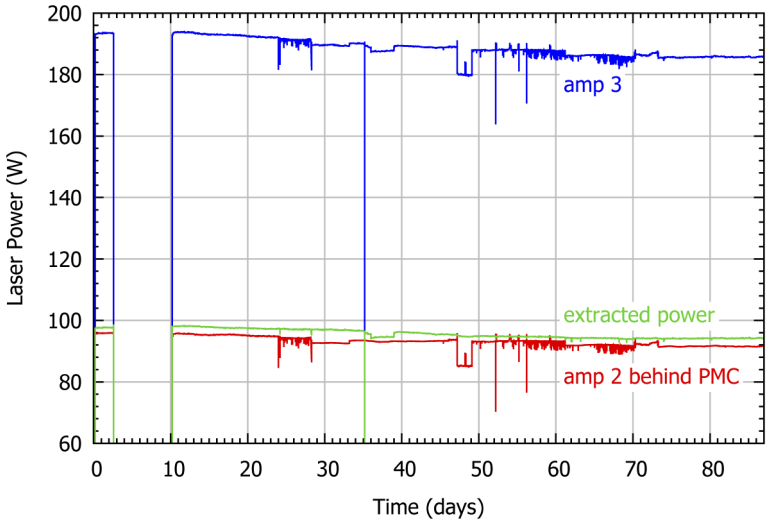

Fig. 4. Output and seed power of the third amplifier as well as the extracted power measured over 88 days. The systems power decreases slightly until it gets to a very stable operation point at about 185 W.

Figure 4 shows an 88 day measurement of the output power of amp 3 in blue, its seed power in red and the difference of both in green. Both time series were measured with calibrated water cooled power meters. A slight drop in both power levels can be observed and at some point both values settle. The times at which an upwards step can be seen in both curves correspond to a manual realignment of the beam coming from amp 2 and going to the PMC. Due to the constant extracted power at high seed powers, we expect that the power of amp 3 changes by the same amount as its seed. However, we see that the power loss of amp 3 is twice the power reduction of

Optics EXPRESS

amp 2 over the full measurement time. This can only be explained by at least partly independent power loss mechanisms as for example due to moving components in front of amp 2 and amp 3 and decreasing diode output power, respectively.

In addition we measured the relative power noise, the frequency noise and the relative pointing of each amplifier. We took these measurements regularly during the long term test and couldn't observe any changes. All measurements were performed at the maximal power levels of 95 W from amp 2 behind the PMC and 195 W from amp 3, respectively. The higher order mode content measured behind amp 3 at this power level was <14%.

Figure 5(a) shows the relative power noise (RPN) as amplitude spectral densities, measured with a high power photo diode in DBB 2.

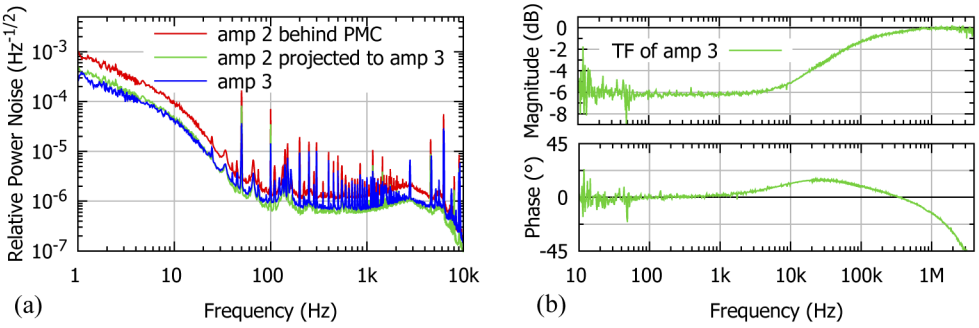

Fig. 5. (a) The relative power noise of amp 3 fits quite well to the seed noise projected to the amplifiers output by means of the measured power noise transfer function. It can be concluded that the RPN of amp 3 is dominated by the seed laser RPN which is attenuated by the frequency dependent amplification of amp 3. (b) The amplifiers transfer function displays the ratio between the RPN of the beam amplified by amp 3 to the RPN of the seed. Its value at low frequencies (≈-6 dB) is equal to the power ratio between seed and amplifier output. At high frequencies the amplification follows the modulation and the gain raises up to a value of 0 dB.

The relative power noise of an amplified laser beam is a combination of the RPN of the seed laser and of the pump diodes. To estimate what fraction of this noise is associated to the power noise of the seed laser, we measured the transfer function from seed laser modulations to output power modulations of amp 3 (Fig. 5(b)). This transfer function shows the expected frequency dependence: at low Fourier frequencies the dynamical processes in the amplifier are fast enough to maintain a steady state situation. Hence, the output power follows the seed power according to the blue measurement points in Fig. 3(b). At higher frequency the inversion of the laser transition is too slow to adapt the the changing seed power. Thus a constant amplifier gain applies and the curve rises to 0 dB (see [17,18] for more details). With this transfer function we projected the measured noise of amp 2 (red curve) to the output power fluctuations of amp 3 (green curve).

If we compare the projected RPN of amp 3 to the actual measurement of the amplifier's RPN in blue we see that the curves are close together, which means that the free running RPN of amp 3 is dominated by the seed laser contribution. The small offset between the curves could be caused by the pump diode's RPN contribution.

The frequency noise measurements of amp 2 behind the PMC and of amp 3 are shown in Fig. 6. For this measurement a dither locking scheme is used to stabilize the length of the triangular cavity in the DBB to the laser frequency [8]. The frequency noise of the laser beam can be calculated from the error and control signal of this feedback control loop. We plot it as an amplitude spectral density. As we would expect from a single pass laser amplifier, the frequency noise of the amplified beam is not higher than that of the seed beam. Both measurement are close to the expected NPRO laser frequency noise projection as can also be seen in Fig. 6. Slight

Optics EXPRESS

offsets between the two curves can most probably be explained by environmental changes that effect the DBB 2 frequency noise measurements.

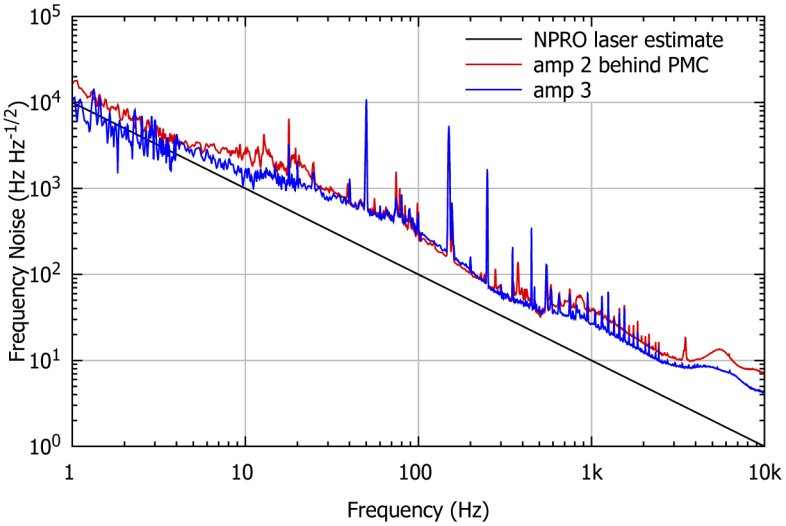

Fig. 6. Frequency noise measurements of amp 2 and amp 3, both measured with DBB 2 behind the PMC. The frequency noise curves of amp 3 and its seed are very similar, which leads to the conclusion, that the third amplifier doesn't add frequency noise to its seed. The small offsets below 30 Hz and above 600 Hz result most likely from environmental changes that effect the DBB measurement.

Measurements of the relative beam pointing noise are presented in Fig. 7. Relative pointing can be defined as the lateral shift between the center of a reference beam and the measured beam at the location of the Gaussian beam waist normalized by the waist radius $\delta x/w_0$ and by the angle between the two beam axes normalized by the divergence angle of the Gaussian beam $\delta\alpha/\theta_D$, both independently in horizontal and vertical direction.

Two quadrant photo diodes (QPDs) and two piezo driven mirrors (PZTs) are used for a differential wave front sensing and automatic alignment scheme of the injected laser to the triangular cavity in the DBB. The four curves per beam pointing measurement are each representing one of the four degrees of freedom, translation and tilt in horizontal and vertical direction at the position of one of the mirrors.

The measurement of the relative pointing noise in Fig. 7 of the second amplifier in front of the PMC was taken with DBB 1 and the other two measurements were performed with DBB 2. For clarity the mean values of the four pointing degrees-of-freedom per measurement were calculated and are highlighted in the figure. The curves for the four independent degrees-of-freedom are plotted in a lighter version of the mean value's color. They deviate less than a factor five from the mean value. When comparing the relative beam pointing noise of amp 2 before and behind the PMC the filtering effect of the PMC can be observed. It should be noted, that this spatial filtering is typically associated with a correlated enhanced power noise in transmission of the PMC. The beam pointing noise measurement of the second amplifier behind the PMC shows reduced noise as expected from this passive filtering. The fact, that the noise is not lower for all frequencies can be due to vibrating optics behind the PMC, as well as sensor noise in the diagnostic breadboard itself.

The pointing of the beam behind the third amplifier is similar to the PMC filtered beam pointing of the second amplifier. Hence, either the amplifier adds this small amount of pointing

Optics EXPRESS

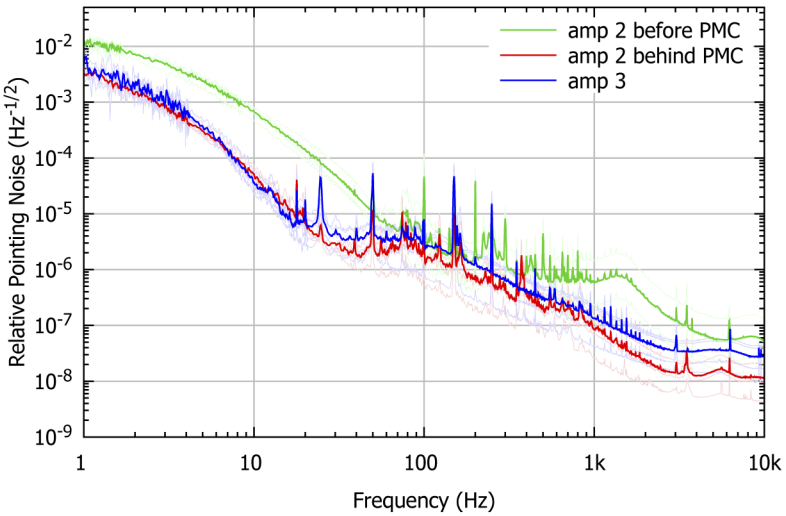

Fig. 7. Relative pointing noise measurements of amp 3 as well as amp 2 measured before and behind the PMC. The curves representing the four independent degrees of freedom for each measurement are plotted in a lighter version of the color used for the corresponding mean values. The low PMC filtered beam pointing is slightly increased when measured behind amp 3, which can be due different environmental conditions between the measurements, that affect the DBB performance.

noise or the small difference is caused by environmental changes that affect the pointing noise measurements.

As mentioned in section 2 the pump diodes and the crystals of the amplifiers are water cooled. As water cooling can cause vibrations on the optical table, as little flow as necessary should be used. To determine the minimal required water flow to cool amp 3 we did DBB measurements with different flow rates. We used water flows from 3l/min down to 0.14l/min to cool the crystals. With decreasing flow we could see that the laser head temperature, as displayed by the control unit, increased from about 21°C to about 26°C, which isn't exceeding the safe operation temperature range, given by the manufacturer. We couldn't measure any dependence of the relative power noise, frequency noise and relative pointing noise on the flow rate in the investigated flow rate interval. Without changing the mode matching and alignment to the amplifier we measured fluctuations in the higher order mode content of ±2.5% and a power loss of 2 W of output power, when decreasing the water flow. The input polarization to amp 3, however had to be slightly readjusted to keep the higher order mode content within this range.

4. Stabilized characterization

In this section we will present the characterization of the third amplifier, when we stabilized the power and frequency of its seed beam, namely the light from the second amplifier after the PMC. As mentioned above we used low power beams leaking from two PMC ports to sense the power and frequency noise for the respective feedback control loop. With an engaged stabilization the measurement accuracy for potential noise added by a neoVAN-4S-HP, in this case of amp 3, can be improved with respect to the results given in section 3. The stabilization scheme that we used for the power and frequency stabilization is similar to the one in the pre-stabilized laser system described in [13]. For the power stabilization a photo diode at one of the low power ports of the PMC was used as sensor. In this setup an acousto optical modulator between the first

Optics EXPRESS

neoVAN-4S-HP and the PMC actuated on the laser power. The resulting power stabilized beam in transmission of the PMC was then used to seed the second neoVAN-4S-HP amplifier (amp 3).

In Fig. 8 the relative power noise of the stabilized beam coming from amp 2 behind the PMC (in red) is shown together with the expected contribution of this noise to the RPN of amp 3 (green) determined via the projection technique described in section 3. Furthermore we show the measured RPN of the amplified light behind amp 3 (blue curve). For comparison we also show again the RPN of amp 3 with free running seed (dashed blue). All measurements were taken with DBB 2. The measured RPN of amp 3 is lower than its RPN when the seed is not stabilized but clearly above the projected RPN contribution of its stabilized seed. This shows that noise is added by this amplifier, which is most likely due to the power noise of its pump diodes.

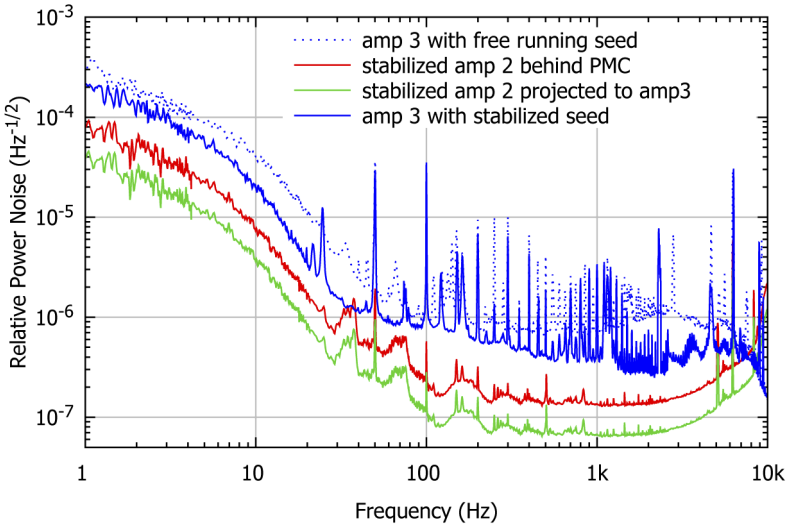

Fig. 8. Relative power noise measurements of amp 3 with free running seed, the stabilized amp 2, the projection of the RPN of amp 2 to the RPN of amp 3 and the measured RPN of amp 3 with stabilized seed. The relative power noise of the second stage is no longer seed dominated, if the seed is stabilized.

Another low power transmissive port of the PMC was used to perform a frequency stabilization. A Pound-Drever-Hall (PDH) locking scheme was used to stabilize the laser frequency to an ultra stable in-vacuum cavity, that served as a frequency reference. (This cavity and the PDH components are not shown in Fig. 1 for clarity. See [13] for a detailed PDH layout). The required phase modulation side bands were produced with an electro-optical modulator (EOM) in between the PMC and the reference cavity and the PDH error signal was generated via a photo diode in reflection of the reference cavity. The control signal was fed back to a piezoelectric element on the NPRO crystal, an EOM right behind the NPRO laser and to the NPRO temperature.

All curves plotted in Fig. 9 were measured with DBB 2. The frequency noise measurement of amp 3 with free running seed is shown in dotted blue. Furthermore we show frequency noise spectral densities of the frequency stabilized amp 2 beam after the PMC (red curve) and of the amp 3 output beam when seeded with this stabilized amp 2 light (blue curve).

The frequency noise curves of the stabilized second amplifier and the third amplifier with stabilized seed are lower than the noise of the third amplifier with free running seed. This shows that the limitation in earlier frequency noise measurements was given by the seed. For Fourier frequencies above 100 Hz the seed and amplifier curve are about the same. Here the measurement is limited either by the frequency stabilization loop or the diagnostic breadboards internal measurement noise, most likely caused by length fluctuations of its reference cavity.

Optics EXPRESS

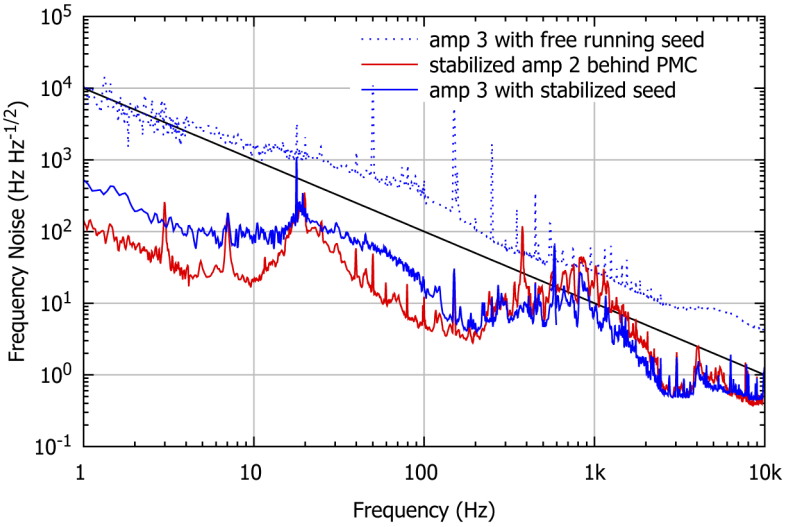

Fig. 9. Frequency noise of the stabilized seed, the projection from the stabilized amp 2 to amp 3 and amp 3 with stabilized seed. The frequency noise of the amp 3 is seed dominated at high frequencies. At low frequencies the frequency noise added by the amplifier is higher than the seeds frequency noise.

Below 100 Hz we see a difference between the two frequency noise measurements. This could be due to the amplifier adding noise to its seed. But it is also possible that the environment and with it the DBB sensor noise is changing over time.

Especially for a power and maybe also for a frequency stabilized seed, we see that the neoVAN-4S-HP adds noise to the amplified beam. Hence, we suggest to include all amplifiers within the feed-back control loop before the corresponding sensor, to not spoil the achieved stability of the pre-stabilized laser system with the added noise of an amplifier behind the pre-stabilization sensing points.

5. Conclusion

In this paper we showed a long term stable laser system based on solid state amplifiers integrated in a pre-stabilized laser environment. The amplifiers are easy to handle and robust against changes in their surroundings. The system delivered an output power of 195 W with a polarization extinction ratio >18 dB and a higher order mode content <14% and therewith is a good option to increase the power of currently operating gravitational wave detector pre-stabilized laser systems.

We showed that the noise added by the second stage of the setup is below the free running noise of the first stage. If the first stage is intensity and frequency stabilized the added noise of the second stage is above the noise of the first stage. Thus we recommend to include all amplifiers in the stabilization feedback control loops to reduce the noise in the output beam send to a gravitational wave detector or other subsequent experiments.

Furthermore, the presented laser amplifiers are good candidates for sub components of laser systems for 3rd generation gravitational wave detectors such as the Einstein Telescope [19] where laser powers exceeding 500 W will be required. Here they could be used as pre-amplifiers for following high power stages or in coherent beam combinations topologies.

Funding

Deutsche Forschungsgemeinschaft (EXC-2123 QuantumFrontiers – 390837967).

Optics EXPRESS

Acknowledgements

We thank Peter Wessels for the useful comments with respect to this manuscript.

Disclosures

The authors declare no conflicts of interest.

References

1. LIGO Scientific Collaboration and Virgo Collaboration, "Observation of Gravitational Waves from a Binary Black Hole Merger," Phys. Rev. Lett. **116**(6), 061102 (2016).
2. LIGO Scientific Collaboration, "Advanced LIGO," Classical Quantum Gravity **32**(7), 074001 (2015).
3. Virgo Collaboration, "Advanced Virgo: a second-generation interferometric gravitational wave detector, Classical Quantum Gravity **32**, 024001 (2014).
4. H. Grote and the LIGO Scientific Collaboration, "The GEO 600 status," Classical Quantum Gravity **27**(8), 084003 (2010).
5. LIGO Scientific Collaboration and Virgo Collaboration, "GWTC-1: A Gravitational-Wave Transient Catalog of Compact Binary Mergers Observed by LIGO and Virgo during the First and Second Observing Runs, Phys. Rev. X **9**, 031040 (2019).
6. LIGO Scientific Collaboration, Virgo Collaboration, Fermi GBM, INTEGRAL, IceCube Collaboration, AstroSatCadmium Zinc Telluride Imager Team, IPN Collaboration, The Insight-Hxmt Collaboration, ANTARES Collaboration,The Swift Collaboration, AGILE Team, The 1M2H Team, The Dark Energy Camera GW-EM Collaboration, theDES Collaboration, The DLT40 Collaboration, GRAWITA: GRAvitational Wave Inaf TeAm, The Fermi Large AreaTelescope Collaboration, ATCA: Australia Telescope Compact Array, ASKAP: Australian SKA Pathfinder, LasCumbres Observatory Group, OzGrav, DWF (Deeper, Wider, Faster Program), AST3, CAASTRO Collaborations, TheVINROUGE Collaboration, MASTER Collaboration, J-GEM, GROWTH, JAGWAR, Caltech- NRAO, TTU-NRAO,NuSTAR Collaborations, Pan-STARRS, The MAXI Team, TZAC Consortium, KU Collaboration, Nordic OpticalTelescope, ePESSTO, GROND, Texas Tech University, SALT Group, TOROS: Transient Robotic Observatory of theSouth Collaboration, The BOOTES Collaboration, MWA: Murchison Widefield Array, The CALET Collaboration,IKI-GW Follow-up Collaboration, H.E.S.S. Collaboration, LOFAR Collaboration, LWA: Long Wavelength Array,HAWC Collaboration, The Pierre Auger Collaboration, ALMA Collaboration, Euro VLBI Team, Pi of the SkyCollaboration, The Chandra Team at McGill University, DFN: Desert Fireball Network, ATLAS, High TimeResolution Universe Survey, RIMAS, RATIR, SKA South Africa/MeerKAT, "Multi-messenger Observations of a Binary Neutron Star Merger," Astrophys. J., Lett. **848**(2), L12 (2017).
7. F. Thies, N. Bode, P. Oppermann, M. Frede, B. Schulz, and B. Willke, "Nd:YVO_4 high-power master oscillator power amplifier laser system for second-generation gravitational wave detectors," Opt. Lett. **44**(3), 719 (2019).
8. P. Kwee and B. Willke, "Automatic laser beam characterization of monolithic Nd:YAG nonplanar ring lasers," Appl. Opt. **47**(32), 6022 (2008).
9. P. Kwee, F. Seifert, B. Willke, and K. Danzmann, "Laser beam quality and pointing measurement with an optical resonator," Rev. Sci. Instrum. **78**(7), 073103 (2007).
10. R. Adhikari, P. Fritschel, and S. Waldman, "Enhanced LIGO," Tech. Rep. LIGO-T060156, LIGO Laboratory (2006).
11. M. Frede, B. Schulz, R. Wilhelm, P. Kwee, F. Seifert, B. Willke, and D. Kracht, "Fundamental mode, single-frequency laser amplifier for gravitational wave detectors," Opt. Express **15**(2), 459 (2007).
12. T. J. Kane and R. L. Byer, "Monolithic, unidirectional single-mode Nd:YAG ring laser," Opt. Lett. **10**(2), 65 (1985).
13. P. Kwee, C. Bogan, K. Danzmann, M. Frede, H. Kim, P. King, J. Põld, O. Puncken, R. L. Savage, F. Seifert, P. Wessels, L. Winkelmann, and B. Willke, "Stabilized high-power laser system for the gravitational wave detector advanced LIGO," Opt. Express **20**(10), 10617 (2012).
14. J. H. Põld, "aLIGO bow-tie Pre-Modecleaner document," Tech. Rep. LIGO-T0900616, Albert-Einstein-Institut Hannover (2012).
15. F. Cleva, J.-P. Coulon, and F. Kéfélian, "Characterization, Integration and Operation of a 100-W Solid State Amplifier in the Advanced-VIRGO Pre-Stabilized Laser System," in *2019 Conference on Lasers and Electro-Optics Europe and European Quantum Electronics Conference*, (Optical Society of America, 2019), pp. 2–4.
16. LIGO Scientific Collaboration, "Instrument science white paper 2019," Tech. Rep. LIGO-T1900409-v3, LIGO Scientific Collaboration (2019).
17. H. Tünnermann, J. Neumann, D. Kracht, and P. Weßels, "Gain dynamics and refractive index changes in fiber amplifiers: a frequency domain approach," Opt. Express **20**(12), 13539–13550 (2012).
18. S. Novak and A. Moesle, "Analytic model for gain modulation in edfas," J. Lightwave Technol. **20**(6), 975–985 (2002).
19. ET Science Team, "Einstein gravitational wave Telescope conceptual design study," Tech. Rep. ET-0106C-10 (2011).